CHEST

A clinicopathological study of lung adenocarcinomas with pure ground-glass opacity > 3 cm on high-resolution computed tomography

Ke Sun[1] · Huikang Xie[2] · Jiabi Zhao[1] · Bin Wang[1] · Xiao Bao[1] · Fei Zhou[3] · Liping Zhang[2] · Wei Li[1]

Abstract

Objectives This study aimed to discuss whether a diameter of 3 cm is a threshold for diagnosing lung adenocarcinomas presenting with radiological pure ground-glass mass (PGGM, pure ground-glass opacity > 3 cm) as adenocarcinomas in situ or minimally invasive adenocarcinomas (AIS-MIAs). Another aim was to identify CT features and patient prognosis that differentiate AIS-MIAs from invasive adenocarcinomas (IACs) in patients with PGGMs.

Methods From June 2007 to October 2015, 69 resected PGGMs with HRCT and followed up for ≥ 5 years were included in this study and divided into AIS-MIA ($n = 13$) and IAC ($n = 56$) groups. Firth's logistic regression model was performed to determine CT characteristics that helped distinguish IACs from AIS-MIAs. The discriminatory power of the significant predictors was tested with the area under the receiver operating characteristics curve (AUC). Disease recurrence was also evaluated.

Results Univariable and multivariable analyses identified that the mean CT attenuation (odds ratio: 1.054, $p = 0.0087$) was the sole significant predictor for preoperatively discriminating IACs from AIS-MIAs in patients with PGGMs. The CT attenuation had an excellent differentiating accuracy (AUC: 0.981), with the optimal cut-off value at −600 HU (sensitivity: 87.5%; specificity: 100%). Additionally, no recurrence was observed in patients manifesting with PGGMs > 3 cm, and the 5-year recurrence-free survival and overall survival rates were both 100%, even in cases of IAC.

Conclusions This study demonstrated that PGGMs > 3 cm could still be AIS-MIAs. When PGGMs are encountered in clinical practice, the CT value may be the only valuable parameter to preoperatively distinguish IACs from AIS-MIAs.

Key Points

• *Patients with pure ground-glass opacity > 3 cm in diameter are rare but can be diagnosed as adenocarcinomas in situ or minimally invasive adenocarcinomas.*

• *The mean CT attenuation is the sole significant CT parameter that differentiates invasive adenocarcinoma from adenocarcinoma in situ or minimally invasive adenocarcinoma in patients with pure ground-glass opacity > 3 cm.*

• *Lung adenocarcinoma with pure ground-glass opacity > 3 cm has an excellent prognosis, even in cases of invasive adenocarcinoma.*

Ke Sun and Huikang Xie contributed equally to this study.
Liping Zhang and Wei Li contributed equally to this study as co-corresponding authors.

✉ Liping Zhang
Lipingzhang2002@163.com

✉ Wei Li
zgshznj@163.com

[1] Department of Radiology, Shanghai Pulmonary Hospital, Tongji University School of Medicine, 507 Zheng Min Road, Shanghai 200433, China

[2] Department of Pathology, Shanghai Pulmonary Hospital, Tongji University School of Medicine, 507 Zheng Min Road, Shanghai 200433, China

[3] Department of Medical Oncology, Shanghai Pulmonary Hospital, Tongji University School of Medicine, 507 Zheng Min Road, Shanghai 200433, China

Abbreviations

AAH	Atypical adenomatous hyperplasia
AIS	Adenocarcinomas in situ
AUC	Area under the curve
DFS	Disease-free survival
GGM	Ground-glass mass
GGN	Ground-glass nodule
GGO	Ground-glass opacity
HRCT	High-resolution computed tomography
HU	Hounsfield unit
IAC	Invasive adenocarcinomas
IASLC/ATS/ERS	International Association for the Study of Lung Cancer/American Thoracic Society/European Respiratory Society
LPA	Lepidic-predominant adenocarcinomas
LVI	Lymphatic/vascular invasion
MIA	Minimally invasive adenocarcinomas
PGGM	Pure ground-glass mass
ROC	Receiver operating characteristic
ROI	Region of interest
SD	Standard deviation
TNM	Tumor, node, and metastasis
VPI	Visceral pleural invasion

Introduction

Pure ground-glass opacity (GGO) is defined as focal nodular lesions of increased attenuation without internal solid components, with the preservation of bronchial and vascular margins on high-resolution computed tomography (HRCT) scans [1]. Numerous studies have focused on pure GGO less than 2.0 or 3.0 cm in diameter; however, no published studies have reported the clinicopathological features of lung adenocarcinoma with radiographically pure GGO with a diameter > 3 cm [2–7]. Previously, we defined pulmonary lesions containing GGO components exceeding 3 cm in diameter as ground glass mass (GGM); thus, pure GGO > 3 cm is subsequently referred to as pure GGM (PGGM) [8].

According to the new international multidisciplinary classification of lung adenocarcinomas published by the International Association for the Study of Lung Cancer (IASLC)/American Thoracic Society (ATS)/European Respiratory Society (ERS), adenocarcinomas consist of different pathological types such as adenocarcinoma in situ (AIS) with pure lepidic growth, minimally invasive adenocarcinoma (MIA) with predominant lepidic growth with ≤ 5 mm invasion, and invasive adenocarcinoma (IAC) with an invasive component > 5 mm [9]. Based on the new classification, the 8th edition of the tumour, node, and metastasis (TNM) staging of lung cancer proposed that AIS-MIA be added to the category of Tis-T1mi, indicating less aggressive behaviour [10]. Notably, one of the most important diagnostic criteria for AIS-MIA (Tis-T1mi) is a nodule size on HRCT less than or equal to 3 cm [9, 10]. With regard to PGGMs larger than 3 cm in diameter, due to the lack of evidence to support that those patients achieve a 100% disease-free survival (DFS) rate, those tumours were classified as lepidic-predominant adenocarcinomas (LPAs, T1a) rather than AIS-MIAs (Tis-T1mi) despite presenting pure lepidic pattern without any invasive component or invasion ≤ 0.5 cm after pathological examination of the whole tumour [9–11].

Previous studies have demonstrated that most pure ground-glass nodules (GGNs) on HRCT correspond frequently to atypical adenomatous hyperplasia (AAH), AIS, and MIA on pathology, which usually show very slow growth during follow-up as well as favourable prognosis [1, 12–14]. However, to our knowledge, no studies have reported an association between the clinical data, including radiological parameters and histopathologic findings, and the prognostic outcomes for patients with lung adenocarcinoma manifesting as PGGMs. Therefore, the purpose of this study was to compare the HRCT characteristics of PGGMs based on histopathological results (AIS-MIA and IAC groups) and to identify significant CT predictors that could distinguish IACs from AIS-MIAs preoperatively. We also investigated the oncologic prognosis of those patients.

Methods and materials

This retrospective study was approved by the Ethics Committee of Shanghai Pulmonary Hospital. The requirement for informed consent was waived.

Study population

Between June 2007 and October 2015, a series of terms, such as "pulmonary GGN" and "GGO" and "sub-solid nodule," were searched by one radiologist (W.L.) in the radiological information system in our hospital, and nearly 14,306 consecutively recruited patients who underwent complete resection and were pathologically confirmed as lung adenocarcinoma were retrospectively studied. A total of 13,385 patients who met the following criteria were excluded: (1) tumour size < 3 cm; (2) preoperative CT scan with contrast enhancement because different CT parameters may cause interpretation bias, especially for CT attenuation; and (3) lost to follow-up or had a follow-up period of less than 5 years. For the remaining 921 subjects with pulmonary GGO > 3 cm, we excluded 852 patients with partially solid GGM. Finally, 69 patients with lesions

representing pure GGO > 3 cm on CT were selected, as shown in Fig. 1.

CT Image acquisition

All patients underwent chest CT examinations before surgery at our institution, and the detailed scanning parameters were as follows. Preoperative CT examination of all patients was required at full inspiration to avoid respiratory motion artefacts. Somatom Definition AS (Siemens Medical Systems) and Brilliance 40 (Philips Medical Systems) scanners were used to scan CT images at an efficient dose of 120 kV tube energy and 200 mAs. The Siemens CT machine used a Somatom Definition AS scanner with 64×0.625 mm detector, 1.0 pitch, and matrix of 512×512. CT images were reconstructed with a thickness of 0.625–1.0 mm, a 0.7-mm increment, and a soft tissue kernel (Siemens B31 filter, Siemens Medical Solutions) by using a medium sharp reconstruction algorithm. The Philips CT machine used a Brilliance 40 scanner with 40×0.625 mm detector configuration, 0.4 pitch, a matrix of 512×512; images were reconstructed at 1.0 mm layer thickness, with 0.7 mm increments, and a sharp reconstruction kernel (C filter, Philips). The mean interval time between CT scans and surgery was 6 days (range: 1–24 days).

Radiological evaluation

The preoperative HRCT scan findings were reviewed by two experienced thoracic radiologists (W.L. and X.B., both with 7 years of work experience). The readings were based on the

lung window setting (window level, −450 Hounsfield units [HU]; width, 1500 HU) and mediastinal window setting (window level, 40 HU; width, 400 HU). Tumour size was measured on the section that displayed the largest diameter of the lesion. The mean CT attenuation (HU) was measured by using region of interest (ROI) cursors, which traced the boundary of the lesions by manually tracing along their inner edge, on slices containing the maximum diameter of the tumours (Fig. 2a) [15]. The lobulated and spiculated margins were defined as a portion of the surface of a lesion that showed a scalloped configuration (Fig. 2d), and fine linear strands extending radially beyond the lesion, respectively. Pleural retraction was defined as a tumour pulling on the pleura and displacing it (Fig. 3g). Discrepancies in measurement and interpretation between observers were resolved by consensus.

Pathological evaluation

All tumours were completely sampled and submitted for microscopic evaluation after surgical resection. Two thoracic pathologists (H.K.X. and L.P.Z., with 16 and 23 years of work experience, respectively) re-evaluated paraffin sections of the entire tumour blinded to the original paraffin section diagnosis and made a final pathological diagnosis based on the new pathological classification criteria of the IASLC/ATS/ERS [9]. A tumour with growth restricted to neoplastic cells along with preexisting alveolar structure (lepidic growth) lacking stromal, vascular, alveolar space, or pleural invasion and tumour necrosis was classified as AIS. A tumour with predominantly lepidic growth and invasive component ≤ 0.5 cm as

Fig. 1 Patient flowchart. Abbreviations: GGO, ground-glass opacity; GGN, ground glass nodule; CT, computed tomography; GGM, ground glass mass (ground-glass opacity > 3 cm); PGGM, pure ground-glass mass
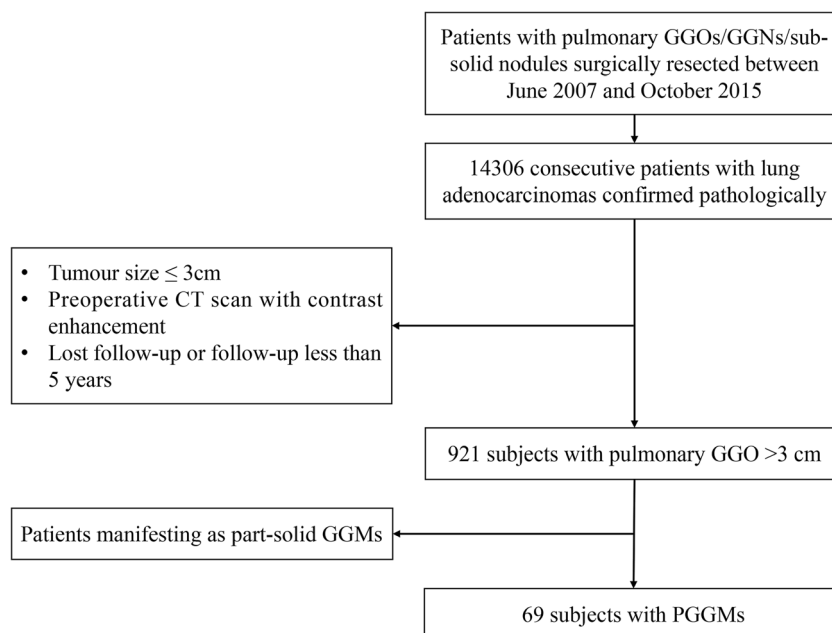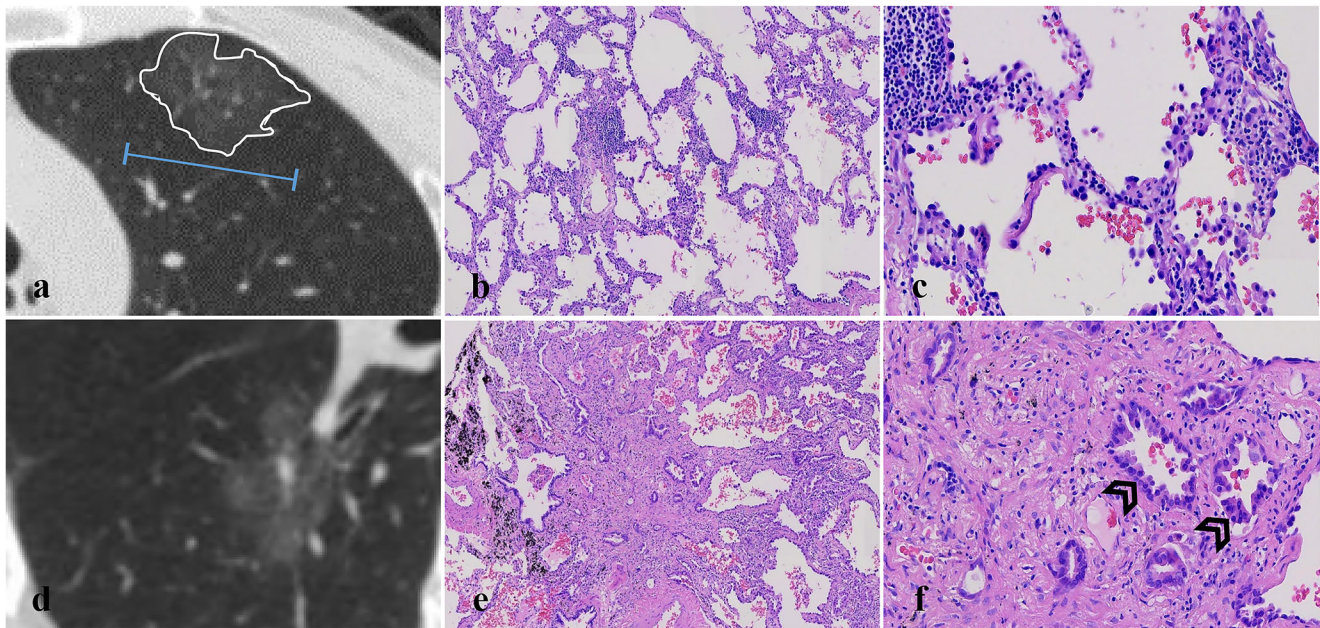
Fig. 2 The measurement method of tumour size and CT attenuation for lung adenocarcinomas manifested as PGGMs. The tumour diameter (blue lines) depended on any planes that could show the maximum size of the lesion, and the mean CT attenuation was automatically measured by delineating the ROI cursors (write contours) on the slice containing the maximum tumour diameter (**a**). **a**–**c** A lobulated marginated PGGM in left upper lobe with a diameter of 3.4 cm. Its mean attenuation value was −740 HU (**a**). Paraffin sections (hematoxylin–eosin stain, original magnification × 100 and × 400, respectively) demonstrated the tumour with growth restricted to neoplastic cells along with preexisting alveolar structure without stromal, vascular, alveolar space, or pleural invasion was diagnosed as AIS (**b**, **c**). **d**–**f** A 3.3 cm PGGM patients with −625 HU CT attenuation (**d**). High-magnification photomicrography supported the diagnosis of MIA because the tumour consisted of predominantly lepidic growth with invasive components (arrowheads) < 0.5 cm, lacking vascular, pleural, or air space invasion (**f**). Abbreviations: CT, computed tomography; PGGM, pure ground-glass mass; ROI, region of interest; HU, Hounsfield units; AIS, adenocarcinoma in situ; MIA, minimally invasive adenocarcinoma

well as lack of vascular, pleural, or air space invasion and tumour necrosis was classified as MIA. The invasive size was measured in the largest dimension. If multiple invasive foci existed simultaneously or the invasive area was difficult to measure, another way was used to estimate the invasive size in which the percentage area of the invasive components was summed and multiplied by the total tumour diameter (i.e., a 4.0 cm tumour with a 10% invasive component would have an estimated invasive size of 0.4 cm) [10]. If the result was no larger than 0.5 cm, a diagnosis of MIA could be considered. Meanwhile, the histological subtypes, pathological nodal involvement, visceral pleural invasion (VPI), and lymphatic/vascular invasion (LVI) were evaluated. Any discrepancies in the measurement interpretation between observers were resolved by consensus.

Follow-up policy

The patients were evaluated at 6-month intervals for the first 2 years, followed by annual check-ups. The follow-up endpoint for this study was set as October 2020. The follow-up evaluation included physical examination, chest radiography, and blood tests, including pertinent tumour markers. Recurrence and survival information was obtained by individual periodic reexamination and readmission (*n* = 50) at our hospital or by telephone interview (*n* = 19). Recurrence was defined as evidence of tumour within the intrapulmonary cavity, hilum or mediastinal lymph nodes, or distant organs.

Statistical analysis

Patients' clinical and CT characteristics were statistically described using the mean ± standard deviation (SD) and frequency (percentage).

The 69 patients were divided into two groups: the AIS-MIA group and the IAC group. Pearson's χ^2 test or Fisher's exact test, as appropriate, for categorical variables and independent samples *t*-test for continuous variables were used when comparing statistical differences between groups.

Due to the small number of eligible patients included, conventional logistic regression was considered unsuitable for assessing associations between variables, which might lead to biased results. In such cases, Firth's logistic regression models were performed to determine significant variables that could be used to distinguish IACs from AIS-MIAs in patients with PGGMs [16, 17]. The variables entered into the multiple regression model were
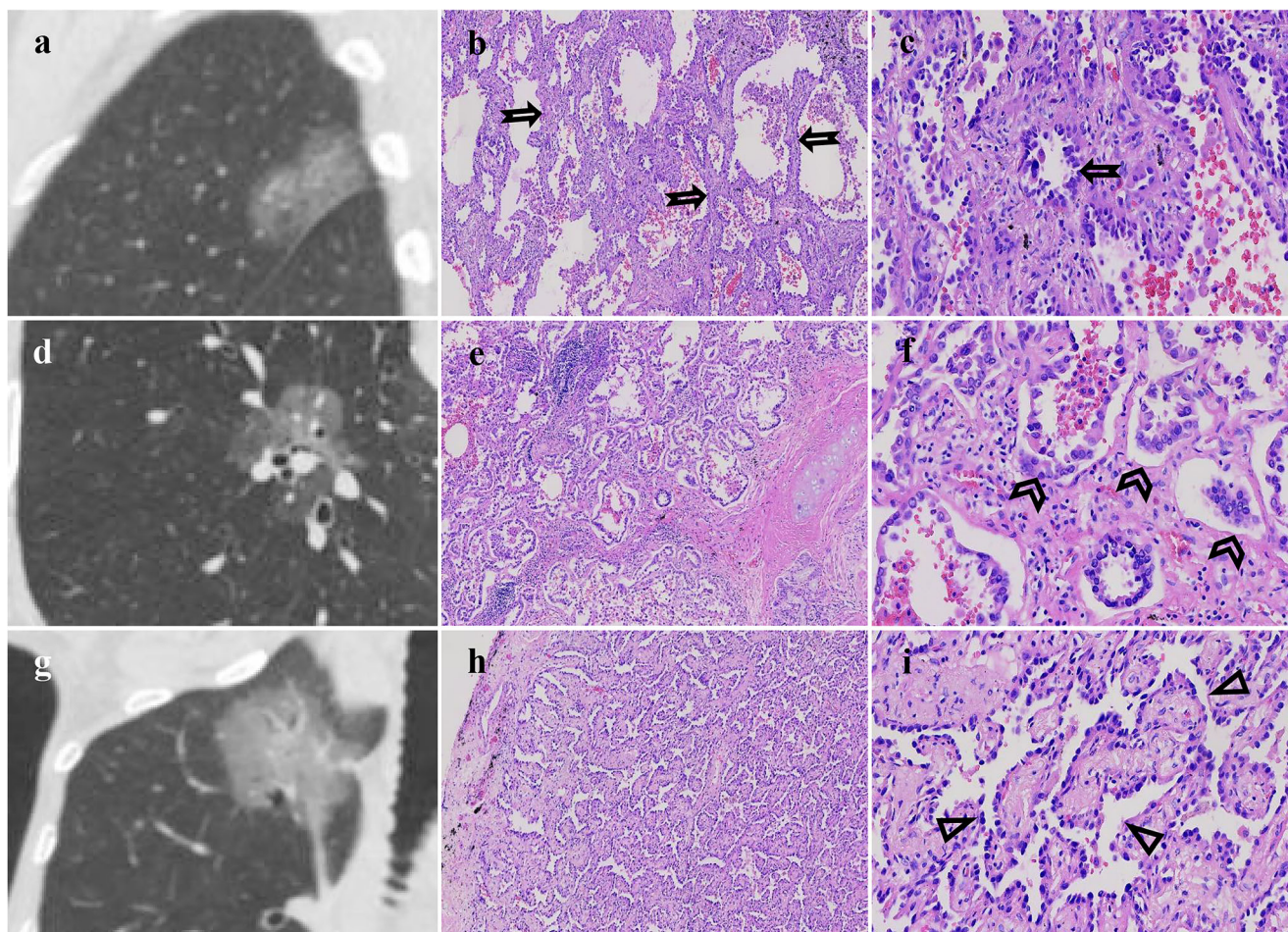
Fig. 3 HRCT features of different pathological subtypes of IACs manifested as PGGMs. **a–c** LPA with a diameter of 3.5 cm and −494 HU CT attenuation showed the subtle lobulated margin (**a**). The paraffin section showed the tumour was LPA (**b**, arrows) and contained the acinar components (**c**, arrow). **d–i** A clear sign of lobulation was found in acinar-predominant IAC. Its size was 3.5 cm and CT attenuation was −480 HU (**d**). Pleural retraction and lobulated margin were evident in a patient with papillary-predominant lung adenocarcinoma whose size and CT attenuation is 4.5 cm and −400 HU, respectively (**g**). Paraffin sections were acinar-predominant (**e**) and papillary-predominant (**h**) IACs, respectively, with representative components of their invasive patterns marked using arrowheads (**f**) and triangles (**i**), respectively. Besides, none of the patients showed lymph node metastasis, LVI, or VPI. Note: Hematoxylin-eosin stain magnification, × 100 for **b**, **e**, and **h**; × 400 for **c**, **f**, and **i**. Abbreviations: LPA, lepidic-predominant adenocarcinoma; LVI, lymphatic/vascular invasion; VPI, visceral pleural invasion

selected based on a p value of less than 0.10 in the univariable analysis and clinical relevance. Furthermore, receiver operating characteristic (ROC) curve and the area under the ROC (AUC) were conducted to evaluate the differentiating capacity of significant CT features.

All statistical analyses were conducted using SAS, version 9.4 (SAS Institute, Inc). Statistical significance was set at p value < 0.05.

Results

Baseline characteristics

The patients' clinicopathological and radiological features are summarised in Table 1. A total of 69 patients had PGGMs

with a tumour size of 3.4 ± 0.4 cm (range: 3.0–4.5 cm). Among them, the average diameters of patient tumours in the AIS-MIA and IAC groups were 3.2 ± 0.1 cm (range: 3.0–3.4 cm) and 3.4 ± 0.4 cm (range: 3.0–4.5 cm), respectively. This study comprised 35 males and 34 females, with a mean age of 61.2 ± 6.9 years. There were 14 ever smokers and 55 never smokers. The locations of the lesions in the patients were as follows: 29 right upper lobes, 2 right middle lobes, 14 right lower lobes, 14 left upper lobes, and 10 left lower lobes. Forty-seven (68.1%) patients had solitary lesions, and 22 (31.9%) had multiple lesions. The mean CT attenuation was −550.6 ± 77.0 HU. Signs of lobulation, spiculation, and pleural retraction were found in 55 (79.7%), 0 (0%), and 25 (36.2%) patients, respectively.

In our study, 8 (11.6%) patients had pathologically proven AIS (Fig. 2a–c), 5 (7.2%) had MIA (Fig. 2d–f), and 56

Table 1 Baseline characteristics in lung adenocarcinoma patients with PGGMs > 3 cm (*n* = 69)

Variables	Patients (%) / value
Age (years)[a]	61.2 ± 6.9
Gender	
Male	35 (50.7)
Female	34 (49.3)
Smoking history	
Ever smoker	14 (20.3)
Never smoker	55 (79.7)
Tumour location	
Right upper lobe	29 (42)
Right middle lobe	2 (2.9)
Right lower lobe	14 (20.3)
Left upper lobe	14 (20.3)
Left lower lobe	10 (14.5)
Lesion number	
Single	47 (68.1)
Multiple	22 (31.9)
Tumour size (cm)[a]	3.4 ± 0.4
Mean CT attenuation (HU) [a]	−550.6 ± 77.0
Lobulated margin	
Presence	55 (79.7)
Absence	14 (20.3)
Spiculated margin	
Presence	0 (0)
Absence	69 (100)
Pleural retraction	
Presence	25 (36.2)
Absence	44 (63.8)
Operation modes	
Lobectomy	66 (95.7)
Segmentectomy	3 (4.3)
Pathological subtypes	
Adenocarcinoma in situ	8 (11.6)
Minimally invasive adenocarcinoma	5 (7.2)
Invasive adenocarcinoma	56 (81.2)
Lepidic-predominant adenocarcinoma	35 (50.7)
Acinar-predominant adenocarcinoma	10 (14.5)
Papillary-predominant adenocarcinoma	11 (15.9)
Lymph metastasis, LVI, and VPI	0 (0)

PGGM, pure ground glass mass (pure ground-glass opacity with the diameter > 3 cm); *HU*, Hounsfield unit

[a] Data are mean ± SD

(81.2%) had IAC. Among 56 IACs, 35 were lepidic predominant adenocarcinomas (LPAs) (Fig. 3a–c), 10 were acinar predominant adenocarcinomas (Fig. 3d–f), and 11 were papillary predominant adenocarcinomas (Fig. 3h–i). Detailed clinical information and CT images of the AIS-MIA group

are displayed in the Supplementary Table and Figures. In addition, none of the patients with PGGMs showed lymph node involvement, VPI, or LVI.

Differences in clinical and radiological features between AIS-MIA and IAC groups

Between the AIS-MIA and IAC groups, significant differences were observed in smoking history (*p* = 0.019), tumour size (*p* = 0.001), mean CT attenuation (*p* < 0.001), lobulated margin (*p* = 0.003), and pleural retraction (*p* = 0.003), as shown in Table 2.

Table 2 The comparison of clinical and radiological features between the AIS-MIA and IAC groups

Variables	AIS-MIA (*n* = 13)	IAC (*n* = 56)	*p* value
Age (years)[a]	61.8 ± 6.2	61.1 (7.1)	0.752
Gender			0.138
Male	9 (69.2)	26 (46.4)	
Female	4 (30.8)	30 (53.6)	
Smoking history			0.019
Ever smoker	6 (46.2)	8 (14.3)	
Never smoker	7 (53.8)	48 (85.7)	
Tumour location			0.695
Right upper lobe	5 (38.5)	24 (42.9)	
Right middle lobe	1 (7.7)	1 (1.8)	
Right lower lobe	3 (23.1)	11 (19.6)	
Left upper lobe	3 (23.1)	11 (19.6)	
Left lower lobe	1 (7.7)	9 (16.1)	
Lesion number			0.096
Single	6 (46.2)	41 (73.2)	
Multiple	7 (53.8)	15 (26.8)	
Tumour size (cm) [a]	3.2 ± 0.1	3.4 ± 0.4	0.001
Mean CT attenuation (HU) [a]	−659.2 ± 45.2	−525.4 ± 58.7	< 0.001
Lobulated margin			0.003
Presence	6 (46.2)	49 (87.5)	
Absence	7 (53.8)	7 (12.5)	
Spiculated margin			
Presence	0 (0)	0 (0)	
Absence	13 (100.0)	56 (100.0)	
Pleural retraction			0.003
Presence	0 (0)	25 (44.6)	
Absence	13 (100.0)	31 (55.4)	

AIS, adenocarcinoma in situ; *MIA*, minimally invasive adenocarcinoma; *IAC*, invasive adenocarcinoma; *HU*, Hounsfield unit

[a] Data are mean ± SD

p value in *t*-test for continuous variables, chi-square test or Fisher's exact test for categorical variables

Table 3 Logistic regression analysis for differentiating IACs from AIS-MIAs in lung adenocarcinomas with PGGM appearance

Variable	Univariable				Multivariable			
	Coefficient	SE	OR	p value	Coefficient	SE	OR	p value
Intercept					32.5864	16.6304		0.0501
Age, years	− 0.0128	0.0444	0.987	0.7735	0.0364	0.0855	1.037	0.6698
Gender (Female)	0.8878	0.6400	2.430	0.1654	− 0.6849	1.5190	0.504	0.6521
Smoking (Presence)	− 1.5982	0.6691	0.202	0.0169	− 2.4870	1.5805	0.083	0.1156
Lesion number (Multiple)	− 1.1281	0.6233	0.324	0.0703	− 1.3383	1.1738	0.262	0.2543
Lobulated margin (Presence)	2.0302	0.6804	7.616	0.0028	0.9809	1.2518	2.667	0.4333
Pleural retraction (Presence)	3.0846	1.4930	21.858	0.0388	− 0.6323	1.6438	0.531	0.7005
Tumour size, cm	2.2208	1.3130	9.214	0.0908	− 0.4334	2.4390	0.648	0.8590
Mean CT attenuation, HU	0.0699	0.0234	1.072	0.0029	0.0522	0.0199	1.054	0.0087
Tumour location (upper lobe)								
Middle lobe	− 1.4319	1.4660	0.239	0.3287				
Low lobe	0.0869	0.6569	1.091	0.8948				

CT, computed tomography; *IAC*, invasive adenocarcinoma; *AIS*, adenocarcinoma in situ; *MIA*, minimally invasive adenocarcinoma; *PGGM*, pure ground-glass mass (pure ground-glass opacity with the diameter > 3 cm); *HU*, Hounsfield unit

Firth's logistic regression analysis for differentiating IACs from AIS-MIAs in lung adenocarcinomas with PGGM appearance

As shown in Table 3, a multivariable logistic regression model revealed that the mean CT attenuation was the sole significant differentiator for IACs from AIS-MIAs (odds ratio: 1.054, $p = 0.0087$).

ROC analysis for the mean CT attenuation

Based on the results of the logistic regression model, a ROC curve analysis was performed to evaluate the differentiating
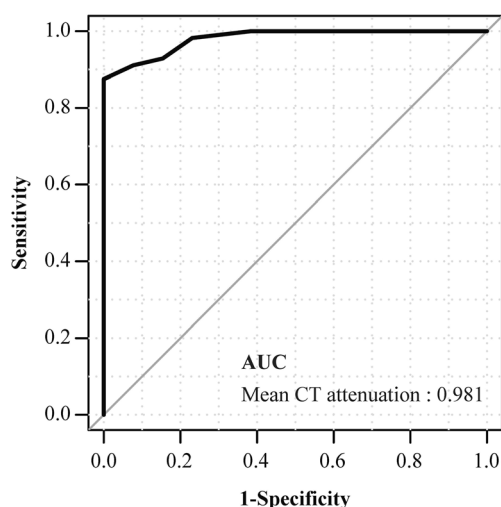

Fig. 4 The ROC curve for the mean CT attenuation found to be significant in PGGMs of different histopathologic groups (AIS-MIA and IAC groups)

capacity of the mean CT attenuation factor. The AUC of the ROC model was 0.981 (95% CI 0.914–0.999) and an optimal cut-off value was identified as −600 HU (Fig. 4). The sensitivity and specificity of this model were 87.5% and 100%, respectively.

Prognosis

The median follow-up period after surgical resection was 70.3 months (range, 60.1–137.4 months), and none of the patients had recurrent disease or metastasis during the follow-up period of at least 5 years.

Discussion

Lung adenocarcinomas manifesting as PGGMs are extremely rare, with a frequency of approximately 0.5% (69/14306). To the best of our knowledge, the present study is the first large study to investigate the HRCT characteristics, histopathological findings, and oncological outcomes of lung tumours presenting as PGGMs. According to the new international multidisciplinary classification of lung adenocarcinomas, one of the criteria for the pathological diagnosis of AIS-MIAs (Tis-T1mi) is tumours with a diameter ≤ 3 cm, whereas radiological PGGMs > 3 cm are classified as LPA (T1a) due to lack of evidence that they have the same 100% DFS rate as AIS-MIAs ≤ 3 cm [9, 10]. In the current study, none of the patients with PGGMs experienced postoperative recurrence or death during the mean 6.4 years of follow-up, and the 5-year RFS rate was 100%. Importantly, 13 of 69 patients were confirmed to have pure lepidic growth or lepidic predominant growth

and had no vascular, pleural invasion, stromal invasion, or invasive component ≤ 5 mm, and no tumour necrosis after pathological examination of the whole tumour. Therefore, these 13 patients could be pathologically diagnosed as AIS/MIAs, even though the tumour diameter was > 3 cm on HRCT scan. In addition, our study also indicated that CT attenuation may be a valuable parameter for the preoperative diagnosis of lung adenocarcinomas with radiological PGGMs > 3 cm as AIS/MIAs; however, this diagnosis should be validated after a comprehensive pathological examination of the whole lesion.

IACs have a relatively high risk for metastasis compared to AIS-MIAs; therefore, it is critical to preoperatively differentiate IACs from AIS-MIAs using HRCT scans. High CT attenuation, larger tumour size, lobulated shape, and pleural retraction are well known radiological findings that are important CT features for distinguishing IACs.

Of the 69 PGGMs, 19% of the lesions were AIS-MIAs, and the mean CT attenuation of these lesions was lower than that of IACs. Increased CT attenuation is an important predictive factor for tumour invasiveness [18]. Previous research revealed a strong negative association between CT attenuation and retained air space in tumours in a study of small peripheral lung adenocarcinomas detected by CT screening [19]. Moreover, these researchers found that the retained air space was larger in noninvasive adenocarcinoma than invasive adenocarcinoma, which was largely due to the increased tumour tissue component and thickened alveolar septa in invasive adenocarcinoma, resulting in reduced air space. These findings suggested that the high CT attenuation of pure GGNs reflected the large number of cells growing along the alveolar septa, which, in terms of the stepwise progression of adenocarcinoma, indicates that the lesion is progressing to invasive adenocarcinoma [20]. Our finding was in accordance with those reported in previous studies. Of the PGGMs, IACs had significantly greater mean CT attenuation than that of AIS-MIAs. Meanwhile, in the results of the logistic regression model, the mean CT value was the single parameter identified as capable of preoperatively distinguishing AIS-MIAs from IACs among PGGMs. Moreover, the cut-off point for the mean CT value in our study was −600 HU, which correlates well with the results of Luo et al, who focused on pure GGNs and reported a cut-off value of −583.6 HU for invasive adenocarcinoma [2]. Furthermore, we found that the specificity of the cut-off value of −600 HU for PGGMs was 100%. Thus, a −600 HU for PGGMs can allow for the complete distinction of IACs from AIS-MIAs and can be used as an appropriate parameter for preoperative prediction of pathological invasiveness in patients with PGGM.

It has been reported that the maximum diameter of the nodule can be a predictor of the histological invasiveness of pure GGNs. Lee et al concluded that pure GGNs with a diameter > 15 mm were more likely to be IACs [3]. Jin X et al reported that for pure GGOs < 3 cm, there were significant differences in nodule size. The mean diameter of IACs was 17.5 mm, which was higher than that of AIS-MIAs [4]. In the study of Lim H et al, tumour size could differentiate between IACs and AIS-MIAs among pure GGNs ≥ 10 mm [5]. The cut-off value was 16.4 mm with a sensitivity and specificity of 61% and 79%, respectively. In our study, the cut-off value of diameter was 3.4 cm for the differentiation of AIS-MIAs from IACs in patients with PGGMs, although the differences were not statistically significant in the multivariable analysis.

A lobulated margin on HRCT generally indicates higher malignancy. However, in our study, the lobulated border was not a significant CT morphologic feature to differentiate IACs from AIS-MIAs manifesting as PGGMs, although lobulation was significantly more frequent in IACs than in AIS-MIAs. Our finding concurred with that of the studies of Lim H et al and Lee et al, in which a non-lobulated border did not prove to be a valuable differentiator among pure GGNs [3, 5]. Similarly, we could not confirm that pleural retraction was a suitable differentiator of IACs from AIS-MIAs manifesting as PGGMs. Furthermore, pathological VPI was not found for PGGMs even though pleural retraction on CT was present. As in Zhao et al's study, lung adenocarcinomas manifesting as pure GGNs less frequently invaded the pleura [6].

The prognosis of IACs presenting as pure GGNs is thought to be excellent [7]. However, the oncological outcomes of PGGMs have not been established. In the present study, although most of the cases were IACs, no recurrence or metastasis was observed in any patients. The 5-year RFS and OS rates for surgically resected PGGMs were both 100% [9]. There are several possible reasons for this finding. It is now well recognised that lung adenocarcinomas with solid or micropapillary predominant subtypes have a higher malignant potential than those with acinar, papillary, and lepidic predominant patterns [21–23]. Furthermore, other studies have shown changes in tumour prognosis when a small micropapillary component (≥ 5%) was present [24, 25]. In our population, we found that all PGGMs on HRCT were pathologically confirmed as nonsolid or non-micropapillary predominant lung adenocarcinomas, and no tumours contained solid or/and micropapillary components. Second, several retrospective studies revealed that lymph node involvement, LVI, and VPI could be more prone to recurrence and metastasis, which leads to poor prognosis [26, 27]. However, in the present study, of the 56 patients with invasive adenocarcinoma, no lymph node metastasis, LVI, or VPI was observed on postoperative pathological analysis.

This study has several limitations that should be considered. First, the small number of patients analysed and the retrospective nature of the analysis may have affected our results. However, we believe that our results reflect the actual clinical practice and can help radiologists and physicians differentiate IACs from AIS-MIAs manifesting as PGGMs in their daily clinical practice. Second, we retrospectively searched for

individuals with pulmonary GGOs, GGNs, or sub-solid nodules identified on CT using the electronic medical records and radiology information system of our hospital, which may lead to selection bias. Third, the mean CT attenuation of PGGMs was evaluated only in the slice containing the part of the lesion with its maximum diameter; thus, this value could potentially be quite different from that of the entire tumour.

In conclusion, the results of this study demonstrated that PGGMs larger than 3 cm could still be AIS-MIAs; additionally, these tumours are not likely to recur within a 5-year follow-up period, even in cases of IAC. When PGGMs are encountered in clinical practice, the mean CT attenuation is a unique valuable parameter to preoperatively distinguish IACs from AIS-MIAs.

Declarations

Guarantor The scientific guarantor of this publication is Wei Li.

Conflict of interest The authors of this manuscript declare no relationships with any companies whose products or services may be related to the subject matter of the article.

Statistics and biometry Aijun You kindly provided statistical advice for this manuscript.

Informed consent Written informed consent was waived by the Institutional Review Board.

Ethical approval Institutional Review Board approval was obtained.

Methodology
• retrospective
• cross-sectional study/diagnostic or prognostic study/observational /
• performed at one institution

References

1. Naidich DP, Bankier AA, MacMahon H et al (2013) Recommendations for the management of subsolid pulmonary nodules detected at CT: a statement from the Fleischner Society. Radiology 266:304–317
2. Zhou QJ, Zheng ZC, Zhu YQ et al (2017) Tumor invasiveness defined by IASLC/ATS/ERS classification of ground-glass nodules can be predicted by quantitative CT parameters. J Thorac Dis 9:1190–1200
3. Lee HY, Choi YL, Lee KS et al (2014) Pure ground-glass opacity neoplastic lung nodules: histopathology, imaging, and management. AJR Am J Roentgenol 202:W224–W233
4. Jin X, Zhao SH, Gao J et al (2015) CT characteristics and pathological implications of early stage (T1N0M0) lung adenocarcinoma with pure ground-glass opacity. Eur Radiol 25:2532–2540
5. Lim HJ, Ahn S, Lee KS et al (2013) Persistent pure ground-glass opacity lung nodules ≥ 10 mm in diameter at CT scan: histopathologic comparisons and prognostic implications. Chest 144:1291–1299
6. Zhao Q, Wang JW, Yang L, Xue LY, Lu WW (2019) CT diagnosis of pleural and stromal invasion in malignant subpleural pure ground-glass nodules: an exploratory study. Eur Radiol 29:279–286
7. Chang B, Hwang JH, Choi YH et al (2013) Natural history of pure ground-glass opacity lung nodules detected by low-dose CT scan. Chest 143:172–178
8. Li W, Zhou F, Wan Z et al (2019) Clinicopathologic features and lymph node metastatic characteristics in patients with adenocarcinoma manifesting as part-solid nodule exceeding 3cm in diameter. Lung Cancer 136:37–44
9. Travis WD, Brambilla E, Noguchi M et al (2011) International Association for the Study of Lung Cancer / American Thoracic Society / European Respiratory Society international multidisciplinary classification of lung adenocarcinoma. J Thorac Oncol 6(2):244–285
10. Travis WD, Asamura H, Bankier AA et al (2016) The IASLC lung cancer staging project: proposals for coding T categories for subsolid nodules and assessment of tumor size in part-solid tumors in the forthcoming eighth edition of the TNM classification of lung cancer. J Thorac Oncol 11:1204–1223
11. Travis WD, Brambilla E, Nicholson AG et al (2015) The 2015 World Health Organization classification of lung tumors. J Thorac Oncol 10:1243–1260
12. Kadota K, Villena-Vargas J, Yoshizawa A et al (2014) Prognostic significance of adenocarcinoma in situ, minimally invasive adenocarcinoma, and nonmucinous lepidic predominant invasive adenocarcinoma of the lung in patients with stage I disease. Am J Surg Pathol 38:448–460
13. Borczuk AC, Qian F, Kazeros A (2009) Invasive size is an independent predictor of survival in pulmonary adenocarcinoma. Am J Surg Pathol 33:462–469
14. Maeshima AM, Tochigi N, Yoshida A, Asamura H, Tsuta K, Tsuda H (2010) Histological scoring for small lung adenocarcinomas 2 cm or less in diameter: a reliable prognostic indicator. J Thorac Oncol 5:333–339
15. Eguchi T, Kondo R, Kawakami S et al (2014) Computed tomography attenuation predicts the growth of pure ground-glass nodules. Lung Cancer 84:242–247
16. Firth D (1993) Bias reduction of maximum likelihood estimates. Biometrika 80:27–38
17. Heinze G, Schemper M (2002) A solution to the problem of separation in logistic regression. Stat Med 21:2409–2419
18. Aoki T, Tomoda Y, Watanabe H et al (2001) Peripheral lung adenocarcinoma: correlation of thin-section CT findings with histologic prognostic factors and survival. Radiology 220:803–809
19. Yang ZG, Sone S, Takashima S et al (2001) High-resolution CT analysis of small peripheral lung adenocarcinomas revealed on screening helical CT. AJR Am J Roentgenol 176:1399–1407
20. Noguchi M (2010) Stepwise progression of pulmonary adenocarcinoma–clinical and molecular implications. Cancer Metastasis Rev 29:15–21
21. Eguchi T, Kadota K, Park BJ, Travis WD, Jones DR, Adusumilli PS (2014) The new IASLC-ATS-ERS lung adenocarcinoma

classification: what the surgeon should know. Semin Thorac Cardiovasc Surg 26:210–222

22. Yanagawa N, Shiono S, Abiko M, Ogata SY, Sato T, Tamura G (2013) New IASLC/ATS/ERS classification and invasive tumor size are predictive of disease recurrence in stage I lung adenocarcinoma. J Thorac Oncol 8:612–618

23. Sasada S, Nakayama H, Miyata Y et al (2015) Comparison of malignant grade between pure and partially invasive types of early lung adenocarcinoma. Ann Thorac Surg 99:956–960

24. Chao L, Yi-Sheng H, Yu C et al (2014) Relevance of EGFR mutation with micropapillary pattern according to the novel IASLC/ATS/ERS lung adenocarcinoma classification and correlation with prognosis in Chinese patients. Lung Cancer 86:164–169

25. Sumiyoshi S, Yoshizawa A, Sonobe M et al (2013) Pulmonary adenocarcinomas with micropapillary component significantly correlate with recurrence, but can be well controlled with EGFR tyrosine kinase inhibitors in the early stages. Lung Cancer 81:53–59

26. Ghaly G, Rahouma M, Kamel MK et al (2017) Clinical predictors of nodal metastases in peripherally clinical T1a N0 non-small cell lung cancer. Ann Thorac Surg 104:1153–1158

27. Aokage K, Miyoshi T, Ishii G et al (2018) Influence of ground glass opacity and the corresponding pathological findings on survival in patients with clinical stage I non-small cell lung cancer. J Thorac Oncol 13:533–542

Publisher's note Springer Nature remains neutral with regard to jurisdictional claims in published maps and institutional affiliations.